

See discussions, stats, and author profiles for this publication at: <https://www.researchgate.net/publication/286735483>

Radiogenic heat production in sedimentary rocks of the Gulf of Mexico Basin, south Texas

Article in AAPG Bulletin · March 1998

CITATIONS

48

READS

329

2 authors:



Thomas E. McKenna

University of Delaware

69 PUBLICATIONS 270 CITATIONS

SEE PROFILE



Jack Sharp

University of Texas at Austin

169 PUBLICATIONS 2,288 CITATIONS

SEE PROFILE

Some of the authors of this publication are also working on these related projects:



Geophysics for Aquifer Characterization [View project](#)



Balmorhea Springs [View project](#)

Radiogenic Heat Production in Sedimentary Rocks of the Gulf of Mexico Basin, South Texas¹

Thomas E. McKenna² and John M. Sharp, Jr.³

ABSTRACT

Radiogenic heat production within the sedimentary section of the Gulf of Mexico basin is a significant source of heat. Radiogenic heat should be included in thermal models of this basin (and perhaps other sedimentary basins). We calculate that radiogenic heat may contribute up to 26% of the overall surface heat-flow density for an area in south Texas. Based on measurements of the radioactive decay rate of α -particles, potassium concentration, and bulk density, we calculate radiogenic heat production for Stuart City (Lower Cretaceous) limestones, Wilcox (Eocene) sandstones and mudrocks, and Frio (Oligocene) sandstones and mudrocks from south Texas. Heat production rates range from a low of $0.07 \pm 0.01 \mu\text{W}/\text{m}^3$ in clean Stuart City limestones to $2.21 \pm 0.24 \mu\text{W}/\text{m}^3$ in Frio mudrocks. Mean heat production rates for Wilcox sandstones, Frio sandstones, Wilcox mudrocks, and Frio mudrocks are 0.88, 1.19, 1.50, and $1.72 \mu\text{W}/\text{m}^3$, respectively. In general, the mudrocks produce about 30–40% more heat than stratigraphically equivalent sandstones. Frio rocks produce about 15% more heat than Wilcox rocks per unit volume of clastic rock (sandstone/mudrock). A one-dimensional heat-conduction model indicates that this radiogenic

heat source has a significant effect on subsurface temperatures. If a thermal model were calibrated to observed temperatures by optimizing basal heat-flow density and ignoring sediment heat production, the extrapolated present-day temperature of a deeply buried source rock would be overestimated.

INTRODUCTION

Hydrocarbon maturation and diagenesis are functions of the thermal history of the host sediments and sedimentary rocks. Numerical modeling is one of the primary tools used to reconstruct this thermal history (Hermanrud, 1993). Although considerable effort has gone into developing sophisticated thermal history models, little effort has gone into quantifying the fundamental thermal rock properties required as model input. Radiogenic heat production of sedimentary rocks is one property that generally has been neglected. To evaluate the thermal history of a sedimentary basin, sources and sinks of heat need to be considered, along with heat transfer via conduction and convection. The source of the heat from the Earth's interior originates from three major sources: (1) primordial energy of planetary accretion, (2) segregation and solidification of the Earth's core, and (3) radiogenic heat production from the decay of uranium (U), thorium (Th), and potassium (K). Although the relative proportions of these sources are uncertain (Durrance, 1986; Pollack et al., 1993), the radiogenic source (in the crust and lithosphere) is estimated to account for about 80% of the heat lost from the Earth's surface (Birch, 1954; Turcotte and Schubert, 1982).

Radiogenic heat production can be divided into three components: heat generated (1) in the lithosphere, (2) in the crust beneath the basin (i.e., basement), and (3) in the sedimentary rocks within the basin. The lithosphere has a low heat-production rate ($0.01 \mu\text{W}/\text{m}^3$ for peridotite), but is a significant heat source per unit surface because of its great thickness. The heat distributed to the base of the crust is dependent on the dynamics of the underlying lithosphere (including aesthenospheric


©Copyright 1998. The American Association of Petroleum Geologists. All rights reserved.

¹Manuscript received June 17, 1996; revised manuscript received February 24, 1997; final acceptance October 21, 1997.

²University of Texas at Austin, Department of Geological Sciences, Austin, Texas 78712. Current address: Delaware Geological Survey, University of Delaware, Newark, Delaware 19716–7501.

³University of Texas at Austin, Department of Geological Sciences, Austin, Texas 78712.

Funding for this project was provided by the office of Basic Energy Research of the U.S. Department of Energy and the Donors of The Petroleum Research Fund, which is administered by the American Chemical Society. We gratefully acknowledge Rich Ketcham and Mark Cloos for access to the α -scintillation counter; Lynton Land, Leo Lynch, and Kitty Milliken for access to their mudrock collection; Larry Mack for analyzing samples to determine the accuracy of our U and Th measurements; and Steve Ingebritsen, Larry Lawver, and the three *Bulletin* reviewers (Stefan Bachu, Dave Blackwell, and John Sclater) for their reviews of this manuscript.

 Data is offered under the AAPG *Bulletin* Datashare program (Data 10). Users can obtain the data set by downloading the file for free from the Internet (<http://www.geobyte.com/download.html>).

upwelling and rifting of the overlying crust), but the heat-flow density at the top of stable continental lithosphere is about 25 ± 10 mW/m² (Durrance, 1986; Fowler, 1990). The lower crust or basement is a more heterogeneous source of heat; average heat production may range from a low of 0.01 μ W/m³ for an ultramafic basement to 10 μ W/m³ for a granitic basement (Roy and Blackwell, 1968; Rybach, 1988). On a local scale, heat production can approach 600 μ W/m³ for a commercial-grade uranium ore. The lithospheric and crustal radiogenic sources, along with convective heat flow into the base of the thermal lithosphere, contribute to what is termed "basement heat-flow density," "basal heat-flow density," or "basement heat flux" (the heat flowing into the base of the sedimentary basin through a unit area). Heat is transferred into the basin by conduction and convection via rock movement (faulting, diapirism, etc.) or fluid flow. Conductive, basal heat-flow density at the lower boundary of a sedimentary basin is typically estimated to be on the order of 15–150 mW/m². Convection of heat from basement to basin fill is difficult to estimate, but may be significant. Within a sedimentary basin, there is a heterogeneous distribution of radioactive minerals. Sedimentary rocks typically generate heat ranging from less than 0.1 μ W/m³ for salt and anhydrite to 5.5 μ W/m³ for "black shale" mudrocks (Rybach, 1986).

In this paper, we quantify heat production in south Texas sedimentary rocks and determine its significance to the overall temperature pattern by calculating the heat produced within the sediments and comparing it to the surface heat-flow density. To simplify the problem and to evaluate the first-order effects of this internal source, we consider one-dimensional, steady-state heat conduction. We do not model sediment deposition, sediment compaction, or convective transport of heat. Sediment deposition and sediment compaction have an effect on temperatures over long periods of time (Sharp and Domenico, 1976), and convective transport of heat has a local effect on temperatures (Bodner and Sharp, 1988; Pfeiffer and Sharp, 1989; McKenna and Sharp, 1996). We evaluate (1) heat production of several stratigraphic units, (2) the quantity of heat generated in the sedimentary sequence, (3) the relationship of heat generated in the sediments to the overall surface heat-flow density, and (4) implications for estimating subsurface temperature.

PREVIOUS WORK AND SIGNIFICANCE

Although radiogenic heat production is recognized as being important, little data have been published on radiogenic heat production of the

sediments within deep basins or on its significance to the overall thermal regime (Keen and Lewis, 1982; Rybach, 1986; Hermanrud, 1993). In a thermal model for the eastern North America divergent margin, Keen and Lewis (1982) calculated that radiogenic heat production in 10 km of sediment contributed about 15% (8 mW/m²) to the total surface heat-flow density of 50–68 mW/m². Calculated temperatures increased up to 17°C at depths of 6 to 10 km in models that included heat production relative to those models where the effect was ignored; the same basal heat-flow density was used in both models. In Keen and Lewis's (1982) study, heat production varied with lithology and ranged from a low of 0.3–0.6 μ W/m³ for limestones to a high of 1.4–1.8 μ W/m³ for shales. Allowing for heat production in the sediments increased the calculated rate of hydrocarbon maturation, and Keen and Lewis's results indicated a maturation date 10–30 m.y. earlier in the source rocks when models included radiogenic heat. Blackwell and Steele (1989) noted that if similar heat-production values were assumed for the Gulf of Mexico basin, radiogenic heat production would contribute from 25 to 50% of surface heat-flow density, but no heat-production data were then available to test their hypothesis. Hermanrud (1993) suggested that radiogenic heat production within the sedimentary sections of basins is generally insignificant, with a contribution of only a few percent or less to heat-flow density. For the Western Canada basin (Alberta, Canada), Bachu (1993) estimated that radiogenic heat production within the sediments ranges from 1 to 22% of the surface heat-flow density.

Measurements of radiogenic heat production in Gulf of Mexico sediments are sparse. The few other observations that have been reported are for pelagic muds (4.3, 4.4, and 4.5 μ W/m³; Epp et al., 1970; Pollack et al., 1993), silty mudstones (1.36 μ W/m³), and carbonates (0.66 μ W/m³) from the deep, central part of the Gulf (Nagihara et al., 1996). No data have been published for the major onshore units of the Gulf of Mexico basin. Host minerals for the volumetrically important radiogenic heat-producing isotopes in the sediments of south Texas are indicated in Table 1. Major sources for U and Th include the heavy minerals apatite, zircon, and monazite, and detrital and authigenic sphene (Milliken, 1988; Milliken and Mack, 1990); noncrystalline forms sorbed onto clay surfaces (Durrance, 1986) as identified by bulk rock analyses of mudrocks (L. S. Land, 1993, personal communication); and organic sources (Durrance, 1986; Bartow and Ledger, 1994). Major K sources include detrital illite and smectite, authigenic illite, and feldspars (Hower et al., 1976; Loucks et al., 1986; Lynch, 1995).

Table 1. Abundances of Naturally Occurring Radioactive Elements in Non-Ore Minerals, Gulf of Mexico Basin*

Mineral	K (wt. %)	U (wt. %)	Th (wt. %)	Mode of Occurrence
Adularia	14.0	-	-	Local cement
Apatite	-	**	**	Detrital
Biotite	8-9	-	-	Detrital
Glaucinite	4.6-6.2	-	-	Detrital
Hornblende	††	-	-	Detrital
Illite/Smectite	0.5-7	-	-	Detrital & authigenic
Microcline	14.0	-	-	Detrital
Monazite	-	†	2-20	Detrital
Muscovite	9.8	-	-	Detrital
Orthoclase	14.0	-	-	Detrital
Sanidine	14.0	-	-	Detrital
Sphene	-	**	**	Detrital & authigenic
Sylvite	52.4	-	-	Evaporitic
Zircon	-	†	†	Detrital

*Average concentrations are from van Schmus (1989) and K. Milliken (1994, personal communication).
**0.001-0.1.
†0.1-0.5.
††0.5-3.

No heat-flow density measurements were published for our study area (Figure 1). Smith et al. (1979) estimated the heat-flow density to be 15 ±3 mW/m² at a depth of 10 km in northern Mexico, about 100 km west of our study area. Nagihara et al. (1996) estimated heat-flow density from the lithosphere (at a subsea depth of 11-13 km) is 40-47 mW/m² in the Sigsbee abyssal plain, about 400 km southeast of the south Texas study area.

Thermal modeling typically is used to predict the timing of hydrocarbon generation. The lack of information on heat production in the sedimentary section poses a problem of accuracy when calibrating these models. Neglecting heat production in the sedimentary section and calibrating a model to observed temperature and surface heat-flow density data may be possible by adjusting the basal heat-flow density and thermal conductivity of the sedimentary section, but this procedure will not necessarily yield an accurate representation of the present-day thermal state of a basin. This point is especially significant when one is using a thermal model to extrapolate temperatures to depths below observations, as is commonly done to determine the present temperature of deeply buried hydrocarbon source rocks. This extrapolated temperature may be the only data point in time for subsequent thermal history modeling of the source rock. Ignoring radiogenic heat production in a model may cause overestimates of present-day temperature. With the thermal maturation rate of organic material in a source rock doubling with every 10°C rise in temperature (Waples, 1980; Lerche, 1990),

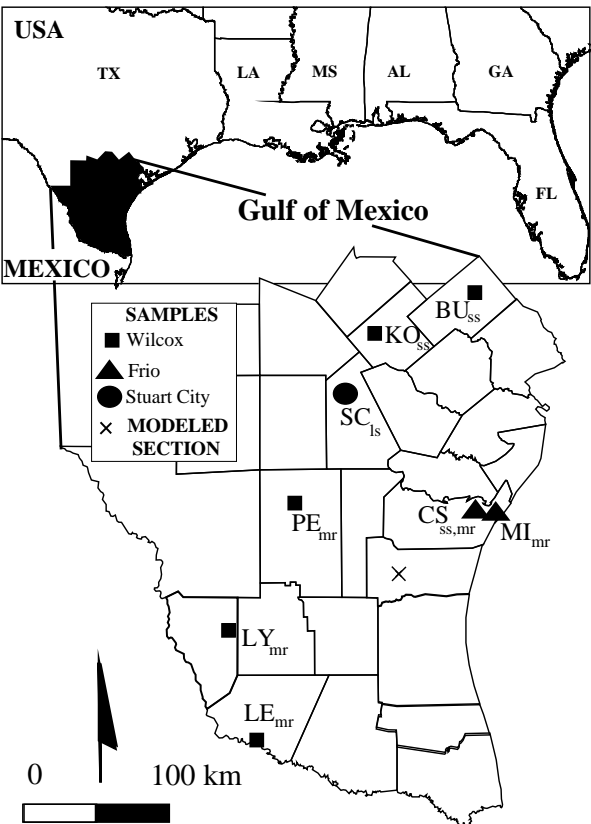


Figure 1—Locations of samples and stratigraphic section. See Table 2 for details on sample locations. Sample name subscripts indicate sample lithology: ss = sandstone, mr = mudrock, ls = limestone.

the calculated rate of hydrocarbon maturation is overestimated, resulting in a premature prediction for the onset of hydrocarbon generation.

METHODOLOGY

We calculated the radiogenic heat production of 100 samples of sandstones, mudrocks, and limestones from south Texas. Rock samples were collected from cores and drill cuttings (Figure 1; Table 2) from the Core Research Center and Department of Geological Sciences collections at the University of Texas at Austin. Additional lithologic and geochemical data for the core samples are available in Stanton (1977), Prezbindowski (1981), Fisher (1982), Lynch (1994), and McKenna et al. (1996). Additional geochemical data for the drill cuttings also were available (L. S. Land, 1995, personal communication). Mudrock samples were hand picked from drill cuttings over approximately 30-m intervals; the depth given in Table 3 is for the midpoint of each interval. We measured α-particle decay rates in an alpha scintillation counter using the method described by Huntley and Wintle (1981), Huntley et al.

Table 2. Sample and Stratigraphic Section Locations

ID	Operator	Well	API No.*	Latitude	Longitude
Wilcox					
BU	Getty	Burns 1	4212330375	29.14°N	97.27°W
KO	Seaboard Oil	Kolodziejczyk 1	4225500897	28.91°N	98.02°W
LY	Shell	Leyendecker 1	4250531222	27.03°N	98.98°W
LE	Shell	H.W. Lehman 1	4242704875	26.38°N	98.85°W
MU	Shell	G. P. Muzza 2	4250531386	27.04°N	98.98°W
Frio					
CS	Cities Services	State Tract 49 2	4235506348	27.77°N	97.30°W
MI	Atlantic Richfield	Mustang Island Deep Unit 1	4235506592	27.74°N	97.15°W
Stuart City					
SC	Tenneco	Schulz 1	4229700141	28.54°N	98.15°W
Stratigraphic Section					
-	Shell	P. Canales 117	4224903809	27.38°N	98.08°W

*API = American Petroleum Institute.

(1986), and Huntley (1988). Counting statistics were used to calculate the concentrations of U and Th as a function of the count rate (Huntley and Wintle, 1981; Daybreak, 1990). U and Th are differentiated by the number of slow pairs detected. A slow pair is defined as two counts occurring within 0.4 s. True pairs result from the decay of ^{216}Po (half life = 0.145 s) in the Th decay chain. These pairs are recorded infrequently and other pairs may be recorded by chance, so the calculated U and Th concentrations are much less precise than the measured rate of α -particle emission. Precision is based on counting statistics, such that the longer the samples are counted, the more precise the measurement. Our experiments concur with those of Huntley (1988), who found that 1000 counts (about 1 day) is an appropriate time limit. Inaccuracy between laboratories and imprecision of count-rate measurements are on the order of 12% for α -particle counts. For assessing accuracy, the isotope dilution method was used at the University of Texas and the neutron activation method was used at XRAL Laboratory (in Ontario, Canada); α -particle counts were calculated based on the U and Th concentrations. Imprecision of U and Th concentrations is on the order of 30%, with the error caused chiefly by the small number of slow pairs counted. To be counted, both pairs must be emitted toward the alpha counter, and occasional pairs will not actually be pairs, but will record two alpha particles from different nuclei that were emitted in the 0.4-s time window of the counter. Huntley (1988) convincingly showed that the α -particle counts can be used directly to estimate heat production without the intermediate step of calculating the concentrations of U and Th; therefore, the imprecision and inaccuracy of our measurements, at most, are 12% of the reported value.

K concentration data were available from ICP spectrometry analyses (L. S. Land, 1995, personal communication) or were measured by the x-ray fluorescence method by XRAL Laboratory. Measurement imprecision and inaccuracy are 5% of the measured value.

We determined bulk density by direct measurements of mass and volume for sandstones and limestones. Mudrock density was established using Dickinson's (1953) curve for Gulf of Mexico mudrocks because desiccation of mudrocks while they were in core storage made accurate direct measurements of in-situ bulk volume and porosity impossible. Measurements of matrix volume via gas porosimetry also failed because minute amounts of water in the mudrocks prevented gas-pressure stabilization in the measurement vessel. Bulk density inaccuracy and imprecision are about 5% of the reported value for sandstone/limestone and 10% of the reported value for mudrock samples.

Heat production is calculated (Rybach, 1986; Huntley, 1988) according to the following equation:

$$A = (\alpha \times a + K \times b) \times \rho_b \quad (1)$$

where A is the bulk-rock heat production rate ($\mu\text{W}/\text{m}^3$), α is the alpha-count rate in number of counts per kilosecond per square centimeter ($\text{counts}/\text{ks}/\text{cm}^2$), a is the conversion factor from the number of alpha particles emitted to the amount of heat produced (equal to $7.288 \times 10^{-4} [\text{mW}/\text{kg}_{\text{solids}}]/[\text{counts}/\text{ks}/\text{cm}^2]$), K is the potassium concentration in weight percent of solids, b is the conversion factor from the percentage of potassium to the amount of heat produced ($3.48 \times$

Table 3. Radiogenic Heat-Production Data for Sedimentary Rocks From South Texas*

Well	No.	Depth (m)	U (ppm)	Th (ppm)	U Error (ppm)	Th Error (ppm)	α Meas. (ct/ks/cm ²)	α Error (ct/ks/cm ²)	K (wt. %)	ρ (kg/m)	A (μ W/m ³)	A Error (μ W/m ³)
Wilcox Mudrocks												
LY	1	4356.5	3.16	11.89	0.88	3.02	0.823	0.019	2.04	2450	1.64	0.18
LY	2	4373.0	2.35	6.50	0.59	2.04	0.528	0.015	0.57	2450	0.99	0.11
LY	3	4373.6	1.89	11.89	0.79	2.71	0.665	0.017	0.57	2450	1.24	0.14
LY	4	4381.8	3.58	8.68	1.00	3.42	0.760	0.023	0.57	2450	1.41	0.16
LY	5	4382.7	2.59	9.54	0.50	1.72	0.667	0.011	0.57	2450	1.24	0.14
LY	6	4389.4	1.87	4.43	0.45	1.54	0.394	0.012	1.90	2450	0.86	0.09
MU	7	4598.7	3.18	9.51	0.40	1.40	0.739	0.009	2.43	2452	1.53	0.16
MU	8	4702.5	3.92	6.73	0.71	2.44	0.730	0.017	1.28	2461	1.42	0.16
MU	9	4709.9	3.27	11.27	0.70	2.41	0.813	0.015	2.37	2461	1.66	0.18
MU	10	4715.3	3.12	11.18	0.59	2.04	0.792	0.012	2.38	2462	1.63	0.18
MU	11	4716.5	3.71	9.59	0.83	2.82	0.808	0.018	2.38	2462	1.65	0.18
MU	12	4728.7	3.36	11.57	0.60	2.07	0.835	0.012	2.81	2463	1.74	0.19
PE	13	4705.4	3.29	13.61	0.79	2.71	0.902	0.016	2.11	2461	1.80	0.20
PE	14	4613.1	4.26	11.60	0.95	3.24	0.948	0.019	2.09	2453	1.87	0.20
PE	15	4466.8	4.49	10.37	1.25	4.26	0.932	0.026	2.01	2450	1.84	0.20
PE	16	4162.0	4.00	8.80	1.22	4.16	0.815	0.026	2.12	2441	1.63	0.18
PE	17	3997.5	3.60	10.20	1.12	3.85	0.817	0.025	2.08	2428	1.62	0.18
PE	18	3832.9	3.33	11.44	1.15	3.95	0.828	0.025	2.12	2425	1.64	0.18
PE	19	3659.1	4.01	9.43	1.09	3.73	0.840	0.023	2.13	2425	1.66	0.18
PE	20	3329.9	3.29	11.37	0.90	3.08	0.819	0.019	2.01	2398	1.60	0.17
PE	21	3165.3	3.30	8.93	0.80	2.75	0.732	0.018	1.84	2385	1.43	0.16
PE	22	3014.5	3.56	9.25	0.83	2.87	0.776	0.018	1.88	2375	1.50	0.16
PE	23	2804.2	3.49	8.34	0.93	3.20	0.735	0.021	1.93	2375	1.43	0.16
PE	24	2648.7	3.93	7.30	0.74	2.52	0.721	0.017	1.86	2367	1.40	0.15
PE	25	2470.4	2.33	12.61	0.94	3.22	0.746	0.020	1.88	2353	1.43	0.16
PE	26	2281.4	3.78	8.39	1.11	3.77	0.772	0.025	2.11	2337	1.49	0.16
PE	27	2107.7	3.79	7.97	1.08	3.71	0.759	0.025	1.88	2323	1.44	0.16
PE	28	1946.1	3.78	10.07	0.87	2.98	0.834	0.019	1.88	2310	1.56	0.17
PE	29	1790.7	3.00	11.13	0.69	2.36	0.774	0.015	1.92	2297	1.45	0.16
PE	30	1641.3	1.98	13.63	1.10	3.78	0.739	0.023	1.86	2285	1.38	0.15
PE	31	1461.5	4.62	7.12	1.21	4.12	0.830	0.027	1.76	2270	1.51	0.17
PE	32	1292.4	4.21	8.16	1.15	3.91	0.818	0.026	2.18	2256	1.52	0.17
PE	33	935.7	3.56	8.37	0.99	3.35	0.745	0.022	2.13	2204	1.36	0.15
PE	34	742.2	4.04	9.27	0.97	3.33	0.836	0.021	2.23	2172	1.49	0.16
LE	35	4327.6	3.41	8.48	0.42	1.47	0.730	0.010	2.03	2450	1.48	0.16
LE	36	4144.8	3.37	9.38	0.79	2.69	0.758	0.017	1.91	2440	1.51	0.17
LE	37	3874.6	3.83	7.30	0.45	1.57	0.739	0.010	1.88	2425	1.47	0.16
LE	38	3701.0	3.23	7.64	0.70	2.42	0.677	0.016	1.96	2425	1.36	0.15
LE	39	3534.6	3.64	8.45	0.89	3.05	0.757	0.020	1.83	2415	1.49	0.16
LE	40	3353.3	3.06	9.85	0.79	2.72	0.736	0.017	1.82	2400	1.44	0.16
LE	41	3169.3	2.29	13.46	1.13	3.88	0.772	0.024	2.02	2385	1.51	0.17
LE	42	3004.7	2.71	10.01	0.81	2.79	0.700	0.018	1.64	2375	1.35	0.15
LE	43	2822.8	3.93	9.10	1.16	3.97	0.817	0.026	1.83	2375	1.57	0.17
LE	44	2627.5	2.96	9.84	0.55	1.88	0.724	0.012	1.72	2366	1.39	0.15
LE	45	2274.1	2.57	12.37	0.08	0.33	0.766	0.005	1.96	2337	1.46	0.16
LE	46	1719.1	2.72	9.86	0.52	1.82	0.694	0.012	1.38	2291	1.27	0.14
LE	47	1544.3	3.56	10.02	1.06	3.64	0.805	0.023	1.55	2277	1.46	0.16
LE	48	5181.6	3.71	8.27	0.63	2.16	0.761	0.014	1.83	2475	1.53	0.17
LE	49	5012.6	3.38	10.30	0.84	2.89	0.792	0.018	1.83	2475	1.59	0.17
LE	50	4842.5	3.98	12.61	0.98	3.37	0.950	0.020	1.83	2472	1.87	0.20
LE	51	4691.3	3.65	12.72	0.75	2.57	0.914	0.015	1.83	2460	1.79	0.20
LE	52	4503.9	3.15	12.68	1.25	4.29	0.852	0.026	1.83	2450	1.68	0.19
LE	53	2099.6	3.70	12.92	0.95	3.24	0.926	0.019	1.96	2322	1.73	0.19
Frio Mudrocks												
MI	54	3861.8	3.35	13.06	0.46	1.62	0.888	0.010	2.09	2425	1.75	0.19
MI	55	4076.7	3.38	12.69	0.88	3.03	0.879	0.018	2.18	2434	1.74	0.19
MI	56	4255.0	4.10	12.50	0.80	2.75	0.961	0.016	2.26	2449	1.91	0.21

Table 3. Continued.

Well	No.	Depth (m)	U (ppm)	Th (ppm)	U Error (ppm)	Th Error (ppm)	α Meas. (ct/ks/cm ²)	α Error (ct/ks/cm ²)	K (wt. %)	ρ (kg/m)	A (μ W/m ³)	A Error (μ W/m ³)
MI	57	4433.3	4.24	11.22	0.85	2.92	0.932	0.017	2.27	2450	1.86	0.20
MI	58	4642.1	3.85	12.67	0.59	2.04	0.936	0.012	2.34	2456	1.88	0.20
MI	59	4826.5	3.72	11.93	0.91	3.12	0.894	0.019	2.21	2471	1.80	0.20
MI	60	5009.4	4.48	10.63	0.98	3.37	0.939	0.020	2.40	2475	1.90	0.21
MI	61	5192.3	3.70	12.89	0.79	2.69	0.925	0.015	2.46	2475	1.88	0.20
CS	62	2663.3	3.52	10.64	0.79	2.70	0.821	0.017	1.48	2370	1.54	0.17
CS	63	2442.7	5.47	4.45	1.17	3.99	0.841	0.027	2.28	2350	1.63	0.18
CS	64	2443.0	4.02	7.19	0.85	2.90	0.759	0.019	2.38	2350	1.50	0.16
CS	65	2443.3	4.08	7.78	0.44	1.53	0.788	0.010	2.31	2350	1.54	0.17
CS	66	2443.6	2.55	13.82	1.24	4.24	0.817	0.026	2.17	2350	1.58	0.17
CS	67	2444.5	3.54	7.28	0.41	1.42	0.702	0.010	2.20	2350	1.38	0.15
CS	68	2598.1	4.47	9.95	1.29	4.37	0.916	0.027	2.22	2350	1.75	0.19
CS	69	2597.8	3.89	10.02	1.35	4.60	0.846	0.029	2.17	2363	1.64	0.18
CS	70	2782.5	6.08	10.94	0.70	2.43	1.151	0.014	2.56	2378	2.21	0.24
Wilcox Sandstones												
BU	71	2929.1	2.71	5.63	0.40	1.36	0.541	0.010	1.10	2300	0.99	0.07
BU	72	2918.2	2.53	5.49	0.55	1.88	0.512	0.014	1.11	2300	0.95	0.06
BU	73	2929.1	2.91	6.05	0.62	2.14	0.580	0.015	0.96	2280	1.04	0.07
BU	74	2845.9	1.17	2.69	0.25	0.86	0.244	0.008	0.52	2210	0.43	0.03
BU	75	2907.6	4.21	2.62	0.62	2.11	0.617	0.016	0.56	2250	1.06	0.07
BU	76	2913.6	1.75	4.25	0.25	0.91	0.367	0.007	0.59	2240	0.65	0.04
KO	77	1592.0	1.53	3.30	0.29	1.03	0.309	0.009	0.90	2540	0.65	0.04
KO	78	1587.1	3.77	4.81	0.33	1.15	0.642	0.008	1.36	2470	1.27	0.08
Frio Sandstones												
CS	79	2747.8	2.90	10.63	0.79	2.71	0.754	0.017	1.30	1795	1.07	0.07
CS	80	2449.1	1.47	4.18	0.32	1.12	0.334	0.009	1.12	2067	0.58	0.04
CS	81	2451.5	4.16	7.82	0.87	2.97	0.800	0.019	2.33	1971	1.31	0.09
CS	82	2452.7	3.36	10.33	1.10	3.78	0.790	0.024	2.03	1977	1.28	0.09
CS	83	2453.3	4.91	9.24	1.31	4.47	0.944	0.028	2.35	1981	1.52	0.10
CS	84	2609.1	3.68	5.30	0.49	1.68	0.648	0.012	2.00	1819	0.99	0.06
CS	85	2609.4	2.92	7.38	0.66	2.28	0.631	0.015	1.83	1861	0.97	0.07
CS	86	2661.5	3.27	12.58	0.62	2.14	0.861	0.013	1.35	1908	1.29	0.08
CS	87	2736.2	3.86	3.97	0.68	2.34	0.623	0.017	1.40	1986	1.00	0.07
CS	88	2737.4	4.78	7.46	0.91	3.13	0.863	0.020	1.88	2028	1.41	0.09
CS	89	2742.3	3.37	10.10	0.54	1.89	0.784	0.012	1.17	1894	1.16	0.08
CS	90	2767.9	4.05	9.81	1.22	4.16	0.859	0.026	1.51	2122	1.44	0.10
CS	91	2745.0	6.89	6.44	1.39	5.16	1.089	0.031	1.20	1832	1.53	0.11
CS	92	2779.9	2.51	7.85	0.40	1.40	0.595	0.010	1.39	1906	0.92	0.06
CS	93	2777.9	4.14	11.84	0.66	2.26	0.942	0.014	1.81	1895	1.42	0.09
CS	94	2783.4	2.57	13.48	0.83	2.82	0.797	0.016	1.30	1903	1.19	0.08
Stuart City Limestones												
SC	95	4094.1	1.67	5.24	0.33	1.14	0.397	0.008	0.58	2640	0.82	0.06
SC	96	4096.5	1.87	7.00	0.56	1.91	0.486	0.014	0.90	2660	1.03	0.07
SC	97	4101.1	0.73	0.06	0.04	0.18	0.094	0.004	0.00	2640	0.18	0.01
SC	98	4117.5	0.35	0.00	0.01	0.00	0.044	0.003	0.00	2550	0.08	0.01
SC	99	4144.7	0.28	0.00	0.01	0.00	0.035	0.003	0.00	2560	0.07	0.01
SC	100	4226.4	0.40	0.00	0.01	0.00	0.052	0.003	0.00	2490	0.09	0.01

*Well = well identification as in Figure 1; No. = unique sample identification number; U = uranium concentration; Th = thorium concentration; U error = error associated with uranium concentration; Th error = error associated with thorium concentration; α = measured α in counts per kilosecond per square centimeter (ct/ks/cm²); α error = error associated with determining measured α in counts per kilosecond per square centimeter (ct/ks/cm²); K = potassium concentration; ρ = bulk density, values for wells 1–70 are estimated from Dickinson (1953); α meas. = measured heat-production rate; α error = error associated with heat production rate.

10⁻⁵ mW/% solids), and ρ_b is the bulk density of the rock (kg/m³). The radiogenic heat production rate is an isotropic petrophysical property

independent of pressure, temperature, and chemical surroundings. Errors propagate in the calculations, and the resulting inaccuracy and

Table 4. Summary Statistics for Measurements of Radiogenic Heat Production*

Rock Type	No.	<i>n</i>	U Mean (ppm)	Th Mean (ppm)	Th/U Mean	K Mean (wt. %)	A Range (μW/m ³)	A Mean (μW/m ³)
Frio mudrocks	54-70	18	4.03	10.57	2.78	2.23	1.23-2.21	1.72
Wilcox mudrocks	1-53	52	3.37	9.91	3.10	1.86	0.86-1.87	1.50
Frio sandstones	79-94	16	3.68	8.65	2.58	1.62	0.58-1.53	1.19
Wilcox sandstones	71-78	8	2.40	4.29	1.98	0.89	0.43-1.27	0.88
Stuart City limestones	95-100	6	0.88	2.05	1.16	0.25	0.07-1.03	-

*No. = unique sample identification number; *n* = number of samples; U mean = mean uranium content in parts per million; Th mean = mean thorium content; Th/U mean = mean of thorium to uranium ratio; K mean = mean potassium content; A range = range of radiogenic heat production; A mean = mean radiogenic heat production.

imprecision are less than 13% of the calculated radiogenic heat production values.

RESULTS OF HEAT PRODUCTION CALCULATIONS

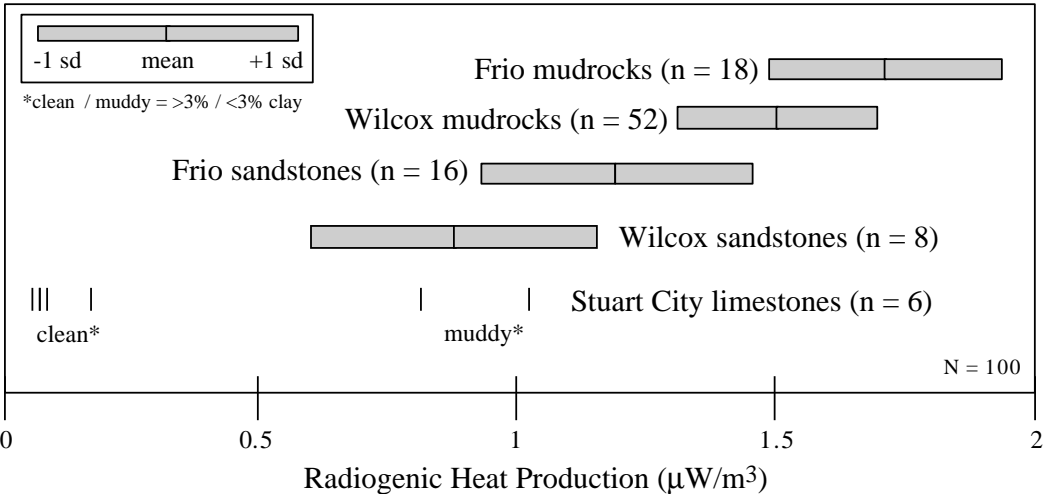
Heat production ranges from a low of 0.07 μW/m³ in clean Stuart City limestones to a high of 2.21 μW/m³ in Frio mudrocks (Table 3). Arithmetic means range from 0.88 μW/m³ for Wilcox sandstones to 1.72 μW/m³ for Frio mudrocks (Figure 2; Table 4). Means were not calculated for the limited limestone data. Mudrocks produce 30-40% more heat than stratigraphically equivalent sandstones, and Frio rocks produce about 15% more heat than Wilcox rocks when they are viewed as a bulk unit of clastic rock (consisting of 80% mudrock and 20% sandstone) (Figures 2, 3). Frio rocks produce more heat because they contain abundant volcanic rock fragments containing higher concentrations of U and Th. Muddy limestones produce heat similar to the sandstones (Figure 2). There may be a small increase in heat production with depth for both

Frio and Wilcox mudrocks (Figure 3) because of the increase in bulk density, but the trend is uncertain due to the 13% error in heat production and the assumed bulk-density function for the mudrocks. No areal trends were identifiable. The heat production that we measured in clean limestones is significantly lower (0.07-0.18) than the typical average (0.62) given in Rybach (1986). Heat production is 5-15% and 20% higher in mudrocks and sandstones, respectively, than in the typical averages (Rybach, 1986), values that exemplify the importance of site-specific measurements.

THERMAL MODELS

We present the results of seven numerical models of one-dimensional, steady-state, conductive heat transport for a 10-km-thick stratigraphic section. The first set of models (models 1-3) is for a true stratigraphic section through the Frio depocenter in south Texas (Figures 1, 4; Table 2). The second set of models (models 4 and 6) and the third set of

Figure 2—Graphical summary of radiogenic heat production data. Arithmetic means and standard deviation (sd) are indicated except for Stuart City limestones (shown as individual samples).



models (models 5 and 7) are for an idealized section composed entirely of Wilcox sandstone, and models 5 and 7 are for an idealized section composed entirely of Frio mudrock. Details on input parameters and constitutive equations are given in Table 5. Porosity is a function of lithology and depth; thermal conductivity is a function of lithology, porosity, and temperature; heat production is a function of lithology (Table 5; Figure 4). Lithology is based on electric logs and geologic interpretations (Sohl et al., 1991; Galloway et al., 1994). Boundary conditions are specified temperature at the top and specified heat-flow density set at the base of the model. We assume the sediment pile is in thermal equilibrium (i.e., no sedimentation-moving boundary effect); this assumption may not be entirely realistic, but this simplification is adequate to quantify the effect of ignoring sediment radiogenic heat production on estimating the present-day temperature of a potential source rock. The only variables modified within a set of models are the amount of radiogenic heat production in the sediment pile and the basal heat-flow density. Model 1 includes sediment heat production, and the basal heat-flow density was optimized to a visual best-fit to observed temperature data. Model 2 neglects heat production and, as in model 1, the basal heat-flow density was optimized to temperature data. Observed temperature data are best estimates based on the suites of Kehle (1971), and are corrected bottom-hole temperatures within 20 km of the stratigraphic section. Model 3 uses the basal heat-flow density determined in model 1, neglects heat production, and is not calibrated to observed temperatures. Models 4 (all sandstone) and 5 (all mudrock) include sediment heat production, and models 6 (all sandstone) and 7 (all mudrock) neglect heat production.

Models 1 and 2 result in optimized basal heat-flow densities of 35 and 45 mW/m², respectively; therefore, a 10 mW/m² higher basal heat-flow density is needed to match the observed temperatures when sediment heat production is ignored. Resulting temperatures at 10 km are 28°C higher in model 2 than in model 1 (Figure 5a); therefore, if sediment heat production were ignored and an optimized higher basal heat-flow density were used to match the observed temperatures, the present-day source rock temperature at 10 km would be overestimated by 28°C. There is most likely some error associated with the temperature observations. If we assume 10°C error bars on the observed temperature data, assume that the thermal conductivity is well constrained, and again optimize the basal heat-flow density, the resulting temperature difference at a depth of 10 km is still higher by about 5°C in the case with no heat production. As the error in the temperature

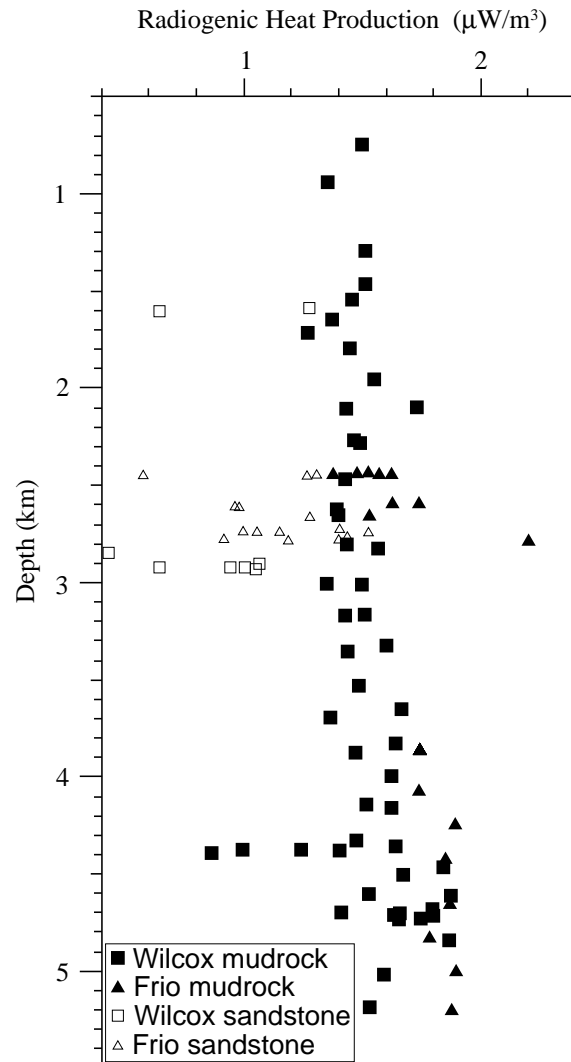


Figure 3—Radiogenic heat production vs. depth for mudrocks and sandstones.

observations goes above 10°C, this effect of radiogenic heat production becomes indiscernible. Comparing model 1 to model 3, it is evident that sediment heat production accounts for 26% of the surface heat-flow density.

For comparative purposes, we also modeled stratigraphic sections consisting entirely of Wilcox sandstone and Frio mudrock (Figure 5b). These serve as end-member simulations for temperature-depth profiles with and without inclusion of heat production. Models 4 (sandstone) and 5 (mudrock) include sediment heat production, and models 6 (sandstone) and 7 (mudrock) neglect heat production. The basal heat-flow density for models 4–7 was assumed to be 45 mW/m², and was not optimized to any temperature observations. For the idealized sandstone section, resulting temperatures in

Table 5. Model Equations, Parameter Descriptions, and Input Values

Equations

Porosity (function of depth) [Sclater and Christie (1980)]

$$\phi = \phi_0 e^{-bz} + \phi_1$$

Thermal conductivity at 20°C (lithology and porosity) [Lewis and Rose (1970)]

$$\lambda_m = \lambda_{ss}^{f_{ss}} \lambda_{mr}^{f_{mr}} \lambda_{ls}^{f_{ls}}$$

$$\lambda_e = \lambda_m^{(1-\phi)} \lambda_w^\phi$$

Thermal conductivity (temperature) [Somerton (1992)]

$$\lambda_{eT} = \lambda_e - 0.001(T - 293)(\lambda_e - 1.38)$$

$$\left[\lambda_e (0.0018T)^{-0.251_e} + 1.28 \right] \lambda_e^{-0.64}$$

Radiogenic heat (lithology)

$$A_m = A_{ss}^{f_{ss}} A_{mr}^{f_{mr}} A_{ls}^{f_{ls}}$$

Model Parameter Descriptions

- ϕ = porosity
- ϕ_0 = surface porosity
- e = effective variable at 20°C
- b = porosity decay term (1/km)
- z = depth (km)
- ϕ_1 = irreducible porosity
- λ = thermal conductivity (W/m/K)
- m = of matrix
- ss = of sandstone
- f = fraction of
- mr = of mudrock
- ls = of limestone
- w = of water
- eT = effective variable at temperature T
- T = temperature (K)
- A = heat production (μW/m³)
- s = at the surface

Model Input Values

Parameter	Wilcox Sandstone	Frio Sandstone	Wilcox Mudrock	Frio Mudrock	Limestone
λ_m	5.8	5.8	1.8	1.8	3.4
A	0.9	1.2	1.5	1.7	0.3
ϕ_0	0.4	0.4	0.55	0.55	0.4
b	0.5	0.5	0.85	0.85	0.5

where
 $\lambda_m = 0.6$
 $T_s = 298$
 $\phi_1 = 0.05$

model 4 (with heat production) at 10 km are 16°C higher than in model 6 (without heat production), and sediment heat production accounts for 17% of the surface heat-flow density. For the idealized mudrock section, resulting temperatures at 10 km are 64°C higher in model 5 (with heat production)

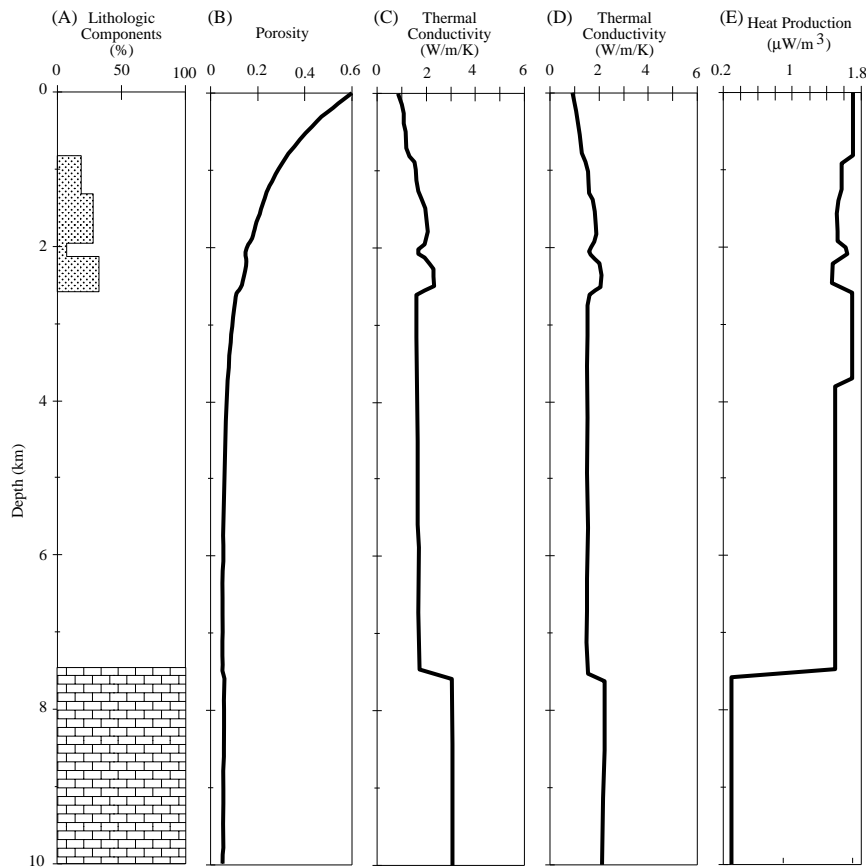


Figure 4—Model parameters with depth calculated from equations from Table 5: (A) lithology (stipple = sandstone, no pattern = mudrock, and “bricks” = limestone), (B) porosity, (C) thermal conductivity as a function of lithology and porosity, (D) thermal conductivity as a function of temperature (assuming $\sim 20^{\circ}\text{C}/\text{km}$ geothermal gradient), and (E) radiogenic heat production.

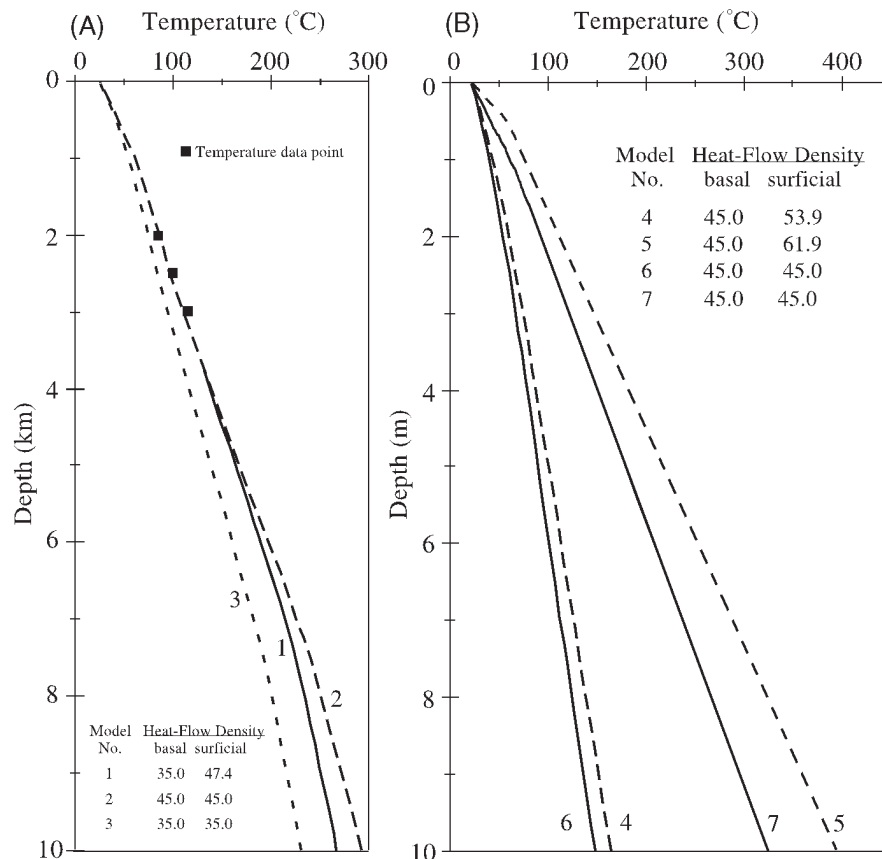
than in model 7 (without heat production), and sediment heat production accounts for 27% of the surface heat-flow density. As expected, radiogenic heat in the mudrock section produces a significantly greater effect on temperature and surface heat-flow density than in the sandstone section.

IMPLICATIONS

Calibrating basal heat-flow density and thermal conductivity to match observed subsurface temperatures is frequently done in thermal modeling. When there are no other thermal indicator data (e.g., vitrinite reflectance, apatite fission-track length) to calibrate the model, the fit to present-day temperatures is the only measure of accuracy of the thermal model. For the eastern North America divergent margin, Keen and Lewis (1982) showed that including radiogenic heat production in modeling resulted in increased temperatures up to 17°C at depths of from 6 to 10 km. Our analysis for south Texas indicates increases in calculated temperature more than 1.5 times that amount (28°C) at 10 km for a simulation

that neglects sediment radiogenic heat production relative to a simulation that considers radiogenic heat production. Our findings are the opposite of the conclusions by Keen and Lewis (1982). The reason for the discrepancy is that the two models we use in our calculation (models 1 and 2) used different basal heat-flow densities that were optimized to match observed temperatures. Keen and Lewis (1982) used the same basal heat-flow density in models that included and that neglected heat production, which is equivalent to comparing our models 1 and 3, which show a similar effect that arises due to the increased amount of heat put into the system by heat production. Our purpose is to show the importance of radiogenic heat production in estimating the present-day temperature of a source rock because this temperature may be the only data point in time for thermal history modeling of the source rock; therefore, by ignoring radiogenic heat production and optimizing basal heat-flow density to temperature observations, thermal maturity may be overestimated and the predicted onset of hydrocarbon generation by subsequent thermal models may be estimated to be earlier than the actual time of generation.

Figure 5—Model results. (A) Results for true stratigraphic section. Squares are temperature data points. Model 1 includes heat production; model 2 neglects heat production. Basal heat-flow density is optimized to fit observations in both models 1 and 2. Model 3 neglects heat production, and basal heat-flow density is not optimized to fit observations. (B) Results for models of idealized sections of all sandstone (models 4 and 6) and all mudrock (models 5 and 7). Models 4 and 5 include sediment heat production; models 6 and 7 neglect heat production.



CONCLUSIONS

Radiogenic heat production within the sedimentary section of the Gulf of Mexico basin is a significant source of heat. We agree with Keen and Lewis (1982) that radiogenic heat production in sediments should be included in thermal history modeling.

(1) Radiogenic heat production within the sedimentary section may contribute up to 26% to the overall surface heat flow in south Texas.

(2) Heat production is greatest in the mudrocks and lowest in the limestones. Mudrocks produce 30–40% more heat than time-equivalent sandstones. Frio rocks produce about 15% more heat than Wilcox rocks as a bulk unit of clastic rock (sandstone/mudrock) because they have higher concentrations of U and Th. Frio sediments contain more volcanic rock fragments than Wilcox sediments.

(3) Radiogenic heat in the sediments has a significant effect on temperatures within the sediments. Ignoring sediment heat production and calibrating a thermal model to temperature observations by optimizing the basal heat-flow density may overestimate the present-day temperature of a potential source rock at 10 km by as much as 28°C.

REFERENCES CITED

- Bachu, S., 1993, Basement heat flow in the Western Canada sedimentary basin: *Tectonophysics*, v. 222, p. 119–133.
- Bartow, P. M., and E. B. Ledger, 1994, Determination of natural radioactivity in Wilcox lignite (Eocene), eastern Texas: *Transactions, Gulf Coast Association of Geological Societies*, v. 54, p. 79–84.
- Birch, F., 1954, Heat from radioactivity, *in* H. Faul, ed., *Nuclear geology: a symposium on nuclear phenomena in the earth sciences*: New York, John Wiley, p. 148–174.
- Blackwell, D. D., and J. L. Steele, 1989, Thermal conductivity of sedimentary rocks: measurement and significance, *in* N. D. Naeser and T. H. McCulloh, eds., *Thermal history of sedimentary basins: methods and case histories*: New York, Springer-Verlag, p. 13–36.
- Bodner, D. P., and J. M. Sharp, Jr., 1988, Temperature variations in south Texas subsurface: *AAPG Bulletin*, v. 72, p. 21–32.
- Daybreak Nuclear and Medical Systems, 1990, Model 582 alpha counter and model 584 printer/controller: Guilford, Daybreak Nuclear and Medical Systems.
- Dickinson, G., 1953, Geological aspects of abnormal reservoir pressure in Gulf Coast Louisiana: *AAPG Bulletin*, v. 37, p. 410–432.
- Durrance, E. M., 1986, *Radioactivity in geology*: New York, John Wiley, 441 p.
- Epp, D., P. J. Grim, and M. G. Langseth, Jr., 1970, Heat flow in the Caribbean and Gulf of Mexico: *Journal of Geophysical Research*, v. 75, p. 5655–5669.
- Fisher, S., 1982, Diagenetic history of Eocene Wilcox sandstones and associated formation waters, south-central Texas: Master's thesis, University of Texas at Austin, Austin, Texas, 185 p.

- Fowler, C. M. R., 1990, *The solid earth*: Cambridge, Cambridge University Press, 472 p.
- Galloway, W. E., X. Liu, D. Travis-Neuberger, and L. Xue, 1994, Reference high-resolution correlation cross sections, Paleogene section, Texas coastal plain: University of Texas at Austin, Texas Bureau of Economic Geology, 19 p.
- Hermanrud, C., 1993, Basin modelling techniques—an overview, in A. G. Dore, J. H. Auguston, C. Hermanrud, D. S. Stewart, and O. Sylta, eds., *Basin modelling: advances and applications*: Norwegian Petroleum Society (NPF) Special Publication 3, p. 1-34.
- Hower, J., E. V. Eslinger, M. E. Hower, and E. A. Perry, 1976, Mechanism of burial metamorphism of argillaceous sediments: 1. Mineralogical and chemical evidence: *Geological Society of America Bulletin*, v. 87, p. 725-737.
- Huntley, D. J., 1988, The use of alpha counting for determining the heat production due to the uranium and thorium decay chains: *Applied Geochemistry*, v. 3, p. 653-656.
- Huntley, D. J., and A. G. Wintle, 1981, The use of alpha scintillation counting for measuring Th-230 and P-231 contents of ocean sediments: *Canadian Journal of Earth Science*, v. 18, p. 419-432.
- Huntley, D. J., M. K. Nissen, J. Thomsen, and S. E. Calvert, 1986, An improved alpha scintillation method for determination of Th, U, Ra-226, Th-230 excess, and Pa-231 excess in marine sediments: *Canadian Journal of Earth Science*, v. 23, p. 959-966.
- Keen, C. E., and T. Lewis, 1982, Measured radiogenic heat production in sediments from continental margin of eastern North America: implications for petroleum generation: *AAPG Bulletin*, v. 66, p. 1402-1407.
- Kehle, R. O., 1971, Geothermal survey of North America, 1971 Annual Progress Report: AAPG Research Committee, 31 p.
- Lerche, I., 1990, Basin analysis, quantitative methods, v. 1: San Diego, Academic Press, 562 p.
- Lewis, C. R., and S. C. Rose, 1970, A theory relating high temperatures and overpressures: *Journal of Petroleum Technology*, v. 22, p. 11-16.
- Loucks, R. G., M. M. Dodge, and W. E. Galloway, 1986, Controls on porosity and permeability of hydrocarbon reservoirs in lower Tertiary sandstones along the Texas Gulf Coast: University of Texas at Austin, Texas Bureau of Economic Geology, Report of Investigations 149, 78 p.
- Lynch, F. L., 1994, Effects of depositional environment and formation water chemistry on the diagenesis of Frio Formation (Oligocene) sandstones: Ph.D. dissertation, University of Texas at Austin, Austin, Texas, 303 p.
- Lynch, F. L., 1995, Illite/smectite in the Frio Formation, part 1: mineralogy and diagenesis in shales and sandstones (abs.): Clay Mineral Society Annual Meeting, Program and Abstracts, p. 84.
- McKenna, T. E., and J. M. Sharp, Jr., 1996, Subsurface pressures, temperatures, and heat transfer in the western Gulf of Mexico basin (abs.): 30th International Geological Congress, Beijing, p. 351.
- McKenna, T. E., J. M. Sharp, Jr., and F. L. Lynch, 1996, Thermal conductivity of Wilcox and Frio sandstones in south Texas (Gulf of Mexico basin): *AAPG Bulletin*, v. 80, p. 1203-1215.
- Milliken, K. L., 1988, Loss of provenance information through subsurface diagenesis, Plio-Pleistocene sandstones, northern Gulf of Mexico: *Journal of Sedimentary Petrology*, v. 58, p. 992-1007.
- Milliken, K. L., and L. E. Mack, 1990, Subsurface dissolution of heavy minerals, Frio Formation sandstones of the ancestral Rio Grande province, south Texas: *Sedimentary Geology*, v. 68, p. 187-199.
- Nagihara, S., J. G. Sclater, J. D. Phillips, E. W. Behrens, T. Lewis, L. A. Lawver, Y. Nakamura, J. Garcia-Abdeslem, and A. E. Maxwell, 1996, Heat flow in the western abyssal plain of the Gulf of Mexico: implications for thermal evolution of the old oceanic lithosphere: *Journal of Geophysical Research*, v. 101, p. 2895-2914.
- Pfeiffer, D. S., and J. M. Sharp, Jr., 1989, Subsurface temperature distributions in south Texas: *Transactions, Gulf Coast Association of Geological Societies*, v. 39, p. 231-245.
- Pollack, H. N., S. J. Hurter, and J. R. Johnson, 1993, Heat flow from the Earth's interior: analysis of the global data set: *Reviews of Geophysics*, v. 31, p. 267-280.
- Prezbindowski, D. R., 1981, Carbonate rock-water diagenesis, Lower Cretaceous, Stuart City trend, south Texas: Ph.D. dissertation, University of Texas at Austin, Austin, Texas, 236 p.
- Roy, R. F., and D. D. Blackwell, 1968, Heat generation of plutonic rocks and continental heat flow provinces: *Earth and Planetary Sciences*, v. 5, p. 1-12.
- Rybach, L., 1986, Amount and significance of radioactive heat sources in rocks, in J. Burrus, ed., *Thermal modeling of sedimentary basins*, Collection Colloques et Seminaires 44: Paris, Editions Technip, p. 311-322.
- Rybach, L., 1988, Determination of heat production rate, in R. Haenel, L. Rybach, and L. Stegena, eds., *Handbook of terrestrial heat-flow density determination*: Dordrecht, Kluwer, p. 125-142.
- Sclater, J. G., and P. A. F. Christie, 1980, Continental stretching: an explanation of the post-mid-Cretaceous subsidence of the central North Sea Basin: *Journal of Geophysical Research*, v. 85, p. 3711-3739.
- Sharp, J. M., Jr., and P. A. Domenico, 1976, Energy transport in thick sequences of compacting sediment: *Geological Society of America Bulletin*, v. 87, p. 390-400.
- Smith, D. L., C. E. Muckerls III, R. L. Jones, and G. A. Cook, 1979, Distribution of heat flow and radioactive heat generation in northern Mexico: *Journal of Geophysical Research*, v. 83, p. 2371-2379.
- Sohl, N. F., E. R. Martinez, P. Salmeron-Urena, and F. Soto-Jaramillo, 1991, Upper Cretaceous, in A. Salvador, ed., *The Gulf of Mexico basin*: Geological Society of America, The Geology of North America, v. J, p. 205-244.
- Somerton, W. H., 1992, Thermal properties and temperature-related behavior of rock/fluid systems: Amsterdam, Elsevier, 257 p.
- Stanton, G. D., 1977, Factors influencing porosity and permeability, Wilcox Group (Eocene), Karnes County, Texas: Ph.D. dissertation, University of Texas at Austin, Austin, Texas, 158 p.
- Turcotte, D. L., and G. Schubert, 1982, *Geodynamics: application of continuum physics to geological problems*: New York, John Wiley, 450 p.
- van Schmus, W. R., 1989, Radioactivity properties of minerals and rocks, in R. S. Carmichael, ed., *Practical handbook of physical properties of rocks and minerals*: Boca Raton, Florida, CRC Press, p. 584-596.
- Waples, D. W., 1980, Time and temperature in petroleum formation: application of Lopatin's method to petroleum exploration: *AAPG Bulletin*, v. 64, p. 916-926.

ABOUT THE AUTHORS

Thomas E. McKenna

Tom is currently a research scientist specializing in hydrogeology at the Delaware Geological Survey, University of Delaware, Newark, Delaware. He completed his Ph.D. in geology at the University of Texas at Austin and earned M.S. and B.S. degrees in geology from the University of South Carolina and Richard Stockton College of New Jersey, respectively. His current research interests include regional hydrogeology, fluid and heat flow in sedimentary basins, applications of GIS (Geographic Information System) technology to geologic problems, and water resources.

**John M. Sharp, Jr.**

John M. (Jack) Sharp is the Chevron Centennial Professor of Geology at the University of Texas at Austin, Austin, Texas. He received a B.S. in geological engineering from the University of Minnesota and his M.S. degree and Ph.D. from the University of Illinois. Sharp is currently studying the thermal evolution of sedimentary basins, regional subsidence along the Gulf Coast, hydrogeology of semiarid zones and alluvial aquifer systems, and fluid flow in fractured rocks and fracture skin analysis.

